European Journal of Pharmaceutics and Biopharmaceutics 89 (2015) 93–106

Contents lists available at ScienceDirect

European Journal of Pharmaceutics and Biopharmaceutics

journal homepage: www.elsevier.com/locate/ejpb

Research paper

Identification and characterization of novel protein-derived arginine-rich cell-penetrating peptides

Ankur Gautam [a], Minakshi Sharma [a], Pooja Vir [a,1], Kumardeep Chaudhary [a], Pallavi Kapoor [a,2], Rahul Kumar [a], Samir K. Nath [b], Gajendra P.S. Raghava [a,*]

[a] Bioinformatics Centre, CSIR-Institute of Microbial Technology, Chandigarh, India
[b] Department of Protein Science and Engineering, CSIR-Institute of Microbial Technology, Chandigarh, India

ARTICLE INFO

Article history:
Received 25 March 2014
Accepted in revised form 24 November 2014
Available online 29 November 2014

Keywords:
Cell-penetrating peptides
Arginine-rich peptides
In silico screening
Macropinocytosis
Uptake efficiency
Intracellular delivery

ABSTRACT

Cell-penetrating peptides (CPPs) have proven their potential as an efficient delivery system due to their intrinsic ability to traverse biological membranes and transport various cargoes into the cells. In the present study, we have identified novel natural protein-derived CPPs using an integrated (*in silico* and experimental) approach. First, using bioinformatics approach, arginine-rich peptide segments were extracted from SwissProt proteins and their cell-penetrating properties were predicted. Finally, eight peptides were selected and their internalization was validated using experimental techniques. Laser scanning confocal microscopy and flow cytometry confirmed that seven out of eight peptides were internalized into live cells with varying efficiencies without significant cytotoxicity. Three peptides have shown higher internalization efficacy than TAT peptide, the most widely used CPP. Among these three peptides, one peptide (P8), derived from voltage-dependent L-type calcium channel subunit alpha-1D, was able to accumulate inside in a variety of cell types very efficiently through a rapid dose-dependent process. Further, experiments involving inhibition with various endocytic inhibitors along with co-localization studies indicate that the uptake mechanism of P8 is macropinocytosis, a fluid-phase endocytosis process. In addition, competitive inhibition with heparin revealed the involvement of cell-surface proteoglycans in P8 uptake. In summary, the present study provides evidence that an integrated *in silico* and experimental approach is an effective strategy for the identification of novel CPPs and CPPs identified in the present study have promising perspectives for future drug delivery applications.

1. Introduction

Most of the therapeutic lead molecules, despite their high therapeutic properties, fail to enter in the clinical trials due to their poor delivery and low bioavailability. Thus considerable efforts have been made to overcome these limitations. In this direction, small cationic peptides known as cell-penetrating peptides (CPPs) have drawn significant attention [1] and provided solutions to the above limitations of poor delivery and low bioavailability. Owing to their intrinsic cell internalization properties, CPPs have improved the intracellular delivery of various therapeutic molecules, including oligonucleotides [2–4], small molecules [5,6], proteins [7], peptides [8], siRNAs [9], nanoparticles [10], etc., most of which otherwise cannot cross the plasma membrane barrier by their own.

The journey of CPP was started almost two decades ago [11] with the discovery of TAT(48–60) [12] and penetratin peptides [13]. Since then hundreds of new CPPs have been discovered [14] and characterized for various therapeutic applications. Recently, a systematic cataloging of these CPPs has been carried out [14], and their analysis has revealed that CPPs constitute a family of diverse peptides; a few CPPs are derived from viral proteins such as VP22 (derived from herpesvirus tegument protein) [15], some are derived from snake venom protein such as CyLOP-1 (derived from crotamine) [16], a few are part of cell adhesion glycoprotein such as pVEC (derived from murine vascular endothelial-cadherin protein), and others are synthetic or designed such as oligoarginine. Though CPPs are very heterogeneous, they share some common features such as CPPs are often cationic, and/or amphipathic in nature [17]. Most of the CPPs are derived from natural proteins

* Corresponding author. Bioinformatics Centre, CSIR-Institute of Microbial Technology, Chandigarh 160036, India. Tel.: +91 172 2690557; fax: +91 172 2690632.
E-mail address: raghava@imtech.res.in (G.P.S. Raghava).
[1] Present address: Public Health Research Institute, New Jersey Medical School, Rutgers, The State University of New Jersey, USA.
[2] Present address: Central Drug Laboratory, Central Research Institute, Kasauli, Himachal Pradesh, India.

http://dx.doi.org/10.1016/j.ejpb.2014.11.020
0939-6411/

Table 1
List of peptides examined.[a]

Designation	Sequence
P1	FITC-ahx-KKKKKKNKKLQQRGD
P2	FITC-ahx-RGDGPRRRPRKRRGR
P3	FITC-ahx-RRRQKRIVVRRRLIR
P4	FITC-ahx-RRVWRRYRRQRWCRR
P5	FITC-ahx-RRARRPRRLRPAPGR
P6	FITC-ahx-LLRARWRRRRSRRFR
P7	FITC-ahx-RGPRRQPRRHRRPRR
P8	FITC-ahx-RRWRRWNRFNRRRCR
TAT	FITC-ahx-GRKKRRQRRRPPQ

[a] All peptides were FITC labeled at the N-terminus. An amino-hexanoic acid linker was placed between the FITC and the peptide. The C-terminus of all peptides is free.

and contain high arginine content, which play crucial roles in mediating their internalization into the cells [18,19]. Despite this heterogeneity in their sequences and structures, CPPs have been suggested to be internalized mainly by endocytosis [20,21]. However, a few CPPs have been reported to be internalized via a non-endocytic process [22,23]. Moreover, internalization mechanism has been shown to be dependent on various factors, including cell types, peptide sequence, peptide concentration, type of conjugated cargo, temperature, incubation time, etc. [24].

Although many CPPs have been identified so far, most of them have shown relatively low uptake efficiencies. Therefore, in the present study, we have used an integrated *in silico* and experimental approache to identify novel and efficient CPPs. To achieve this, first, using bioinformatics approach; we have extracted arginine-rich segments (length 15 amino acid) in all the proteins available in SwissProt database. Subsequently, various filters were applied to define CPPs. To further achieve higher success rate, cell-penetrating properties of peptides were predicted using CellPPD [25], an *in silico* algorithm for the CPP prediction, recently developed by our group. Finally, eight predicted peptides were selected (Table 1) and their cell-penetrating properties were validated experimentally on human epithelial cervical carcinoma cells (HeLa) cells using fluorescence-activated cell sorting (FACS) and confocal-laser scanning microscopy (CLSM). Results demonstrate that seven out of eight peptides internalized into live cells with varying efficiencies without significant toxicities. Three peptides internalized more efficiently than the TAT peptide, a widely used intracellular delivery vehicle. Among these, one peptide derived from human voltage-dependent L-type calcium channel subunit alpha-1D (P8, RRWRRWNRFNRRRCR) was found to be approximately 10 times more efficient than TAT and it internalized into the live cells very efficiently via an endocytic process, making P8 a promising candidate for further molecular and cellular investigations. This investigation also provided a validation of the prediction algorithm to identify new CPP sequences.

2. Material and methods

2.1. Materials

Human cervical cancer cell line HeLa, human prostate carcinoma cell line PC3, human normal prostate epithelium cell line RWPE-1 and Chinese hamster ovary cell line CHO-K1 were all obtained from American Type Culture Collection (ATCC; Manassas, VA). Dulbecco's Modified Eagle's Media (DMEM), RPMI-1640, Ham's F12 nutrient mix, Keratinocyte-SFM, fetal bovine serum (FBS), trypsin, penicillin, streptomycin, Opti-MEM, phosphate buffer solution (PBS, pH 7.4), Tetramethylrhodamine-dextran 70 kDa (marker for macropinocytosis), Tetramethylrhodamine-transferrin (marker for clathrin-coated pits and vesicles), LysoTracker RED (marker for lysosomes), DAPI (marker for nucleus) and antifade reagent were purchased from Molecular Probes (Eugene, OR). Methyl-β-cyclodextrin (MβCD), chlorpromazine (CPZ), cytochalasin D (CytD), amiloride, sodium azide and 2-deoxyglucose (DOG), heparin and fluorescein isothiocyanate (FITC) were purchased from Sigma–Aldrich (USA). MTS cell proliferation assay kit was purchased from Promega (Madison, USA). All the peptide synthetic reagents were procured from Sigma–Aldrich (USA).

2.2. Methods

2.2.1. Peptide synthesis

All CPPs were synthesized by solid phase peptide synthesis strategy using Fmoc (N-(9-fluronyl)-methoxycarbonyl) chemistry in 0.01 mmole scale on a Protein Technologies Inc, USA, PS-3 peptide synthesizer. Fmoc-amino acid was loaded on 2-Chlorotrityl chloride resin manually and then chain elongation was done on the synthesizer and mass was confirmed by MALDI-TOF. In brief, Fmoc-amino acid, 2 equiv., was anchored on 2-Chlorotrityl chloride resin (substitution 1.01 mmole/g, 100–200 mesh, 1%DVB) manually using diisopropylethylamine (5 equiv.) in dichloromethane. Free 2-Chlorotrityl chloride linkers were capped by the treatment of the resin with a solution of dichloromethane (DCM)/methanol/diisopropylethylamine (17:2:1; v/v/v) twice and subsequently with a solution of dimethylformamide (DMF)/diisopropylethylamine/acetic anhydride (8:1:1; v/v/v) twice. After this, the resin was washed three times each with DMF and DCM respectively and finally dried in vacuum for 4 h. The chain elongation of the peptide was done by using four equiv. of the protected Fmoc-amino acid with HBTU (2-(1H-Benzotriazole-1-yl)-1,1,3,3-tetramethyluronium hexafluorophosphate) as a coupling reagent and HOBT (n-hydroxybenzotriazole) or COMU (1-Cyano-2-ethoxy-2-oxoethylidenaminooxy) dimethylamino-morpholino-carbenium hexafluorophosphate) for suppressing racemization with 1 h reaction time. Following side chain protection was employed for Fmoc-protected amino acids, Asparagine, Glutamine, Histidine, Serine: Trityl (trt); Glutamic acid, Aspartic acid: Tert butyl ester (OtBu); Arginine: 2,2,4,6,7-Pentamethyldihydrobenzofuran-5-sulfonyl (Pbf); Lysine, Tryptophan: tert-butoxycarbonyl (Boc); Threonine, Tyrosine: tert-butyl (tBu). For C-terminal activation, 0.4 M NMM in DMF was used and for N-terminal Fmoc-group deprotection, 20% piperidine in DMF was used. COMU was used specifically when two or more hydrophobic amino acids occur in succession in the sequence to have better yield. Reaction time was increased from 1.0 h to 1.5 h during coupling of hydrophobic amino acids. The completion of the reaction was monitored by performing Kaiser Test.

2.2.2. Peptide labeling with FITC and purification

N-terminal of the peptide(s) was attached to a spacer amino acid Fmoc-ε-amino hexanoic acid to avoid fluorescent thiohydantoin (FTH) formation from the last α-amino acid of the peptide sequence. Final Fmoc-group was removed with 20% piperidine in DMF for 15 min twice and was thoroughly washed with DMF six times. Then the resin was swelled with DCM and drained. Prepared 1:1 equivalent of FITC dye in pyridine/DMF/DCM (12:7:5) and 500 μl of the solution was added to the resin and mixed it for overnight. Completion of the labeling was checked by performing Kaiser Test. After the completion of the reaction, the resin was washed with DMF twice, isopropanol twice, DCM twice and dried on a vacuum. Thereafter, the peptide was cleaved from the resin by treating the resin with a cleavage cocktail Trifluoroacetic acid/1,2-Ethanedithiol/water/Thioanisole/phenol/Triisopropylsilane (89:2.5:2.5:2.5:2.5:1, v/v/v/v/v/v) for 6 h. Then it was filtered, dried under air pressure and subsequently on a vacuum to yield

14–18 mg of the crude peptide. Crude peptide was purified by Dionex Ultimate 3000 HPLC on a reverse phase C-18 (4.6 × 250 mm) column using water/acetonitrile gradient containing 0.1% Trifluoroacetic acid. Then from the pure eluting fraction, organic solvent was evaporated and lyophilized to complete dryness yielded 10–12 mg of the purified peptide. Masses of the peptide(s) were confirmed by MALDI-TOF. A summary of all synthesized peptides is provided in Table 1.

2.2.3. Cell culture

PC3 and CHO-K1 cells were grown in Ham's F12 medium supplemented with 10% FBS and L-glutamine (2 mM). HeLa cells were cultured in DMEM, supplemented with 10% FBS and 1% penicillin/streptomycin antibiotics. RWPE-1 cells were cultured in Keratinocyte-SFM medium supplemented with human recombinant epidermal growth factor (5 ng/ml) and bovine pituitary extract (0.05 mg/ml). All cells were maintained at 37 °C in humidified 5% CO_2 atmosphere.

2.2.4. Quantification of cellular uptake

To quantify the FITC-labeled peptide uptake, HeLa cells (2.0×10^5 per well) were seeded at 37 °C onto 24-well plates approximately 24 h before the start of experiments. Thereafter, cells were washed with PBS and incubated in the presence of FITC-labeled peptides (10 μM each) in complete medium for 1 h at 37 °C. Following the above treatment, cells were washed with PBS (2×) to remove the excess extracellular unbound peptides. Subsequently, cells were rinsed twice with heparin (100 μg/ml) and incubated with trypsin (1 mg/ml) for 10 min to remove non-internalized surface bound peptides. Following this, cells were centrifuged at 1000 rpm for 5 min, washed and finally suspended in PBS. FITC fluorescence intensity of internalized peptides in live cells was measured by flow cytometry using Accuri C6 flow cytometer (BD Biosciences) by acquiring 10,000 live cells. Experiments were carried out twice in triplicate. Data were obtained and analyzed using CFlow Sampler (BD Biosciences). The error bars indicate the standard error and untreated cells in media alone were used as controls.

2.2.5. Effect of ATP depletion and low temperature on the uptake of peptide

To analyze the uptake of peptides at low temperature, HeLa cells were maintained at 4 °C for 30 min followed by incubation with FITC-labeled peptides (5 μM) at 4 °C for additional 30 min. Similarly, to analyze the uptake of peptide under ATP depleted conditions, HeLa cells were pretreated with 0.1% sodium azide and 50 mM DOG for 30 min in Opti-MEM followed by incubation with FITC-labeled peptide (5 μM) in the presence of sodium azide and DOG for further 30 min. Thereafter, cells were washed with PBS (2×), heparinized/trypsinized and suspended in PBS. Uptake was measured by flow cytometry as described above and compared with parallel uptake at 37 °C.

2.2.6. Effect of endocytosis inhibitors

To measure the effect of various endocytosis inhibitors on the uptake of P8 peptide, HeLa cells were pretreated for 30 min at 37 °C, in Opti-MEM, with (i) 30 μM CPZ; (ii) 10 μM CytD; (iii) 5 mM amiloride; and (iv) 5 mM MβCD. Thereafter, cells were incubated with FITC-labeled peptide (5 μM each) in the presence of each inhibitor for additional 30 min in Opti-MEM. The effect of the drugs was verified, in parallel control experiments, by analyzing the cellular uptake of tetramethylrhodamine labeled transferrin, a known marker of clathrin-mediated endocytosis, and tetramethylrhodamine labeled Dextran, a marker of macropinocytosis (data not shown).

In order to evaluate the effect of heparin on the cellular uptake of P8, HeLa cells were pretreated at 37 °C for 30 min in Opti-MEM with 10 μg/ml heparin, followed by incubation with the FITC-labeled P8 peptide (5 μM) in the presence of heparin (10 μg/ml) for 30 min at 37 °C. At the end of incubation, cells were washed with PBS, rinsed with heparin (100 μg/ml) and treated with trypsin (1 mg/ml) for 10 min at 37 °C. Uptake of the peptide was analyzed by flow cytometry as described above.

2.2.7. Cell uptake visualization studies by live cell imaging

In order to visualize the FITC fluorescence and distribution of internalized peptides, HeLa cells (1×10^5 cells) were seeded onto 12-well plates containing 16 mm glass coverslips, 24 h prior to incubation with FITC-labeled peptides. After complete adhesion, the cell culture medium was replaced with fresh medium containing FITC-labeled peptides (10 μM each), and then the cells were incubated at 37 °C for 1 h. Cells were not fixed to avoid artifactual localization of the internalized peptides [26]. At the end of the incubation period, culture medium was removed and coverslips were washed thoroughly with PBS (3×, 2 min) and mounted on glass slides with antifade reagent. Localization of FITC-labeled peptides in the live cells (unfixed) was analyzed immediately using Nikon A1R confocal microscope.

For co-localization studies, HeLa cells, grown on coverslips, were incubated with either LysoTracker Red (100 nM) or tetramethylrhodamine Dextran-70 (70 kDa, 200 μg/ml) along with FITC-labeled-P8 (5 μM) in serum free medium for 1 h at 37 °C. Thereafter, cells were washed with PBS (3×) and immediately examined using confocal microscope.

2.2.8. Structural analysis of peptides

The tertiary structures of all peptides were predicted by PEPFOLD [27], which is a *de novo* approach for prediction of peptide structure. In addition, secondary structure states of these peptides have been assigned from predicted tertiary structures using software DSSP [28]. Helical wheel projection analysis of peptides was performed using the pepwheel function of EMBOSS (http://www.sacs.ucsf.edu/Documentation/emboss/pepwheel.html).

2.2.9. CD spectroscopy

CD spectra of TAT and P8 (100 μM each) were recorded using a nitrogen-flushed Jasco spectropolarimeter using a 0.1 cm quartz cell with a bandwidth of 2 nm and a scan speed of 50 nm/min. Spectra of TAT and P8 were recorded in the water, 90% 2,2,2-trifluoroethanol (TFE) and SDS micellar solution (CMC = 8.2 mM). Each spectrum was the average of five scans with background of the water subtracted.

2.2.10. Cellular toxicity of peptides

The toxicity of peptides was assessed using MTS cell proliferation assay (CellTiter $96^{®}_{AQueous}$ Non-Radioactive Cell Proliferation Assay, Promega) according to the manufacturer's protocol. In brief, HeLa cells were seeded at a density of 5×10^3 cells/well in 96-well microtiter plates in DMEM supplemented with 10% FBS 24 h before the start of the experiment. Cells were incubated with different concentrations (5, 10, 20, 40, and 80 μM, respectively) of unlabeled peptides for 24 h. Control cells did not receive any peptide treatment. At the end of the incubation period, MTS assay reagents were added. Cells were placed back into the 37 °C humidified atmosphere with 5% CO_2 for 4 h and the absorbance was measured at 490 nm with an infinite F200 plate reader (Tecan Systems Inc.). The survival of cells relative to the control (cells incubated with growth medium containing no peptide) was calculated by taking the ratio of the absorbance at 490 nm (A_{490}) values. All the experiments were performed in triplicates.

3. Results

3.1. In silico approach for identification of potential CPPs

It has been seen that the majority of CPPs discovered so far, are derived from natural proteins. Most of these peptides are polycationic in nature and consist of multiple Arg residues that confer cell-penetrating properties. Therefore, we considered it very likely that many arginine-rich cryptic CPP sequences within the primary sequences of SwissProt proteins should have intrinsic cell internalizing properties. In order to discover novel potential and efficient CPP candidates, we have used an *in silico* approach to identify all possible arginine-rich sequences in SwissProt proteins (Fig. 1). It has previously been shown that eight/nine arginine residues are optimum for efficient internalization of oligo-arginines [29]. Therefore, peptide segments of window length 15 with eight/nine arginine (~53–60% arginine content) that produce an overall high positive charge were searched in SwissProt proteins. As a result, a total 12,053 sequences satisfying the above-mentioned criteria were fished out and among which 7680 were found to be unique (Fig. 1).

Since most of the CPPs are not cell type specific, therefore, in order to identify CPPs, which can be selective to cancer cells, a filter was applied to identify peptides having the tumor homing motif RGD (Arg, Gly, Asp) at N-terminus. RGD motif has high affinity toward integrin receptors [30,31], which are often overexpressed on tumor cells during tumor progression and play an important role in tumor angiogenesis. This screening has resulted into 12 peptides, which have RGD motif at N-terminus. For rest 7668 peptides, we used CD-HIT software [32] to remove peptides having similarity more than 60%, which resulted into 421 significant different peptides. In order to achieve a higher success rate, the resultant 421 peptides were submitted to CellPPD webserver to predict cell-penetrating properties. CellPPD is an *in silico* algorithm [25], which gives an SVM score for each peptide submitted to the server. Higher the SVM score, higher will be the probability of a given sequence to be a CPP. Based upon SVM scores, we further selected 356 peptides having SVM scores more than 0.50, demonstrating high probabilities of these peptides to be CPPs. Since it has been observed that negatively charged residues such as Asp and Glu are usually less preferred in CPPs [14,25]; we applied a filter to remove all peptides having these negatively charged residues. Remaining peptides were then scanned for the presence of RXXR motif at C-terminus. It has been previously shown that peptides with exposed RXXR motif at C-terminus (C-end Rule) were internalized into tumor cells by binding to neuropilin receptor [33], which is overexpressed on the surface of most of the cancer cells. This screening resulted into three datasets as shown in Fig. 1. Seven peptides were selected for experimental validation of cell penetrating properties. From dataset 1, we selected one peptide (P2) having RGD at N-terminus and RXXR motif at C-terminus. From datasets 2 and 3, we selected four (P3, P6, P7, P8) and two

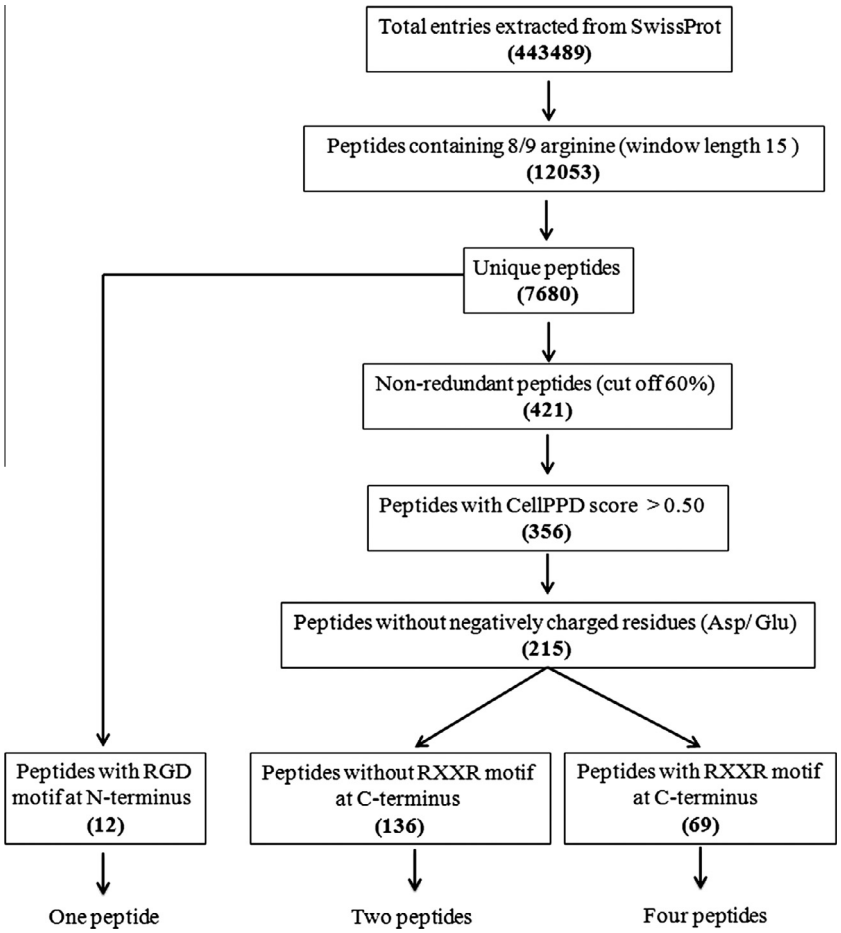

Fig. 1. *In silico* approach for identification of natural protein-derived cell-penetrating peptides. All entries from SwissProt were extracted and 15 amino acid length peptides containing nine arginine residues were fished out. Various filters such as scanning of peptides for the presence of tumor homing motif (RGD), prediction using CellPPD algorithm and presence of tumor penetrating motif (RXXR, C-end Rule) were applied to find out potential CPPs. Finally, seven peptides were selected for experimental validation.

peptides (P4 and P5), respectively. Since it has been suggested that arginine is crucial and preferred over lysine in cell penetration [29], we have selected one lysine-rich natural protein-derived peptide (P1) just to compare the efficiency of this lysine-rich peptide with arginine-rich peptides. Sequences of these selected peptides and the SwissProt IDs of their corresponding proteins are summarized in Table 2. All these peptides are derived from different species, including human, rat, *Mycobacterium tuberculosis*, mouse, viruses and *Arabidopsis thaliana*.

3.2. Quantification of cellular uptake of predicted peptides

Next, we wanted to evaluate whether shortlisted predicted CPP candidates have intrinsic ability to internalize into live cells. Therefore, these peptides were synthesized, labeled with FITC and their uptake efficiencies were analyzed by FACS. A well-known CPP, TAT(48–60) was used as a control to compare the efficiency of these peptides.

Table 3 shows the amino acid sequences and charge of the examined peptides. All peptides have almost similar charge (+8 to +9) and arginine content (8–9 arginine) except P1, which has 8 lysine residues. Some of these peptides also contain tryptophan and proline residues. HeLa cells were treated with FITC-labeled peptides (10 μM) for 60 min at 37 °C in complete medium followed by flow cytometry analysis as described in materials and methods. Before analysis, cells were treated with heparin (100 μg/ml) and trypsin (1 mg/ml) just to remove any externally surface-bound non-internalized peptide [26]. Fig. 2 demonstrates the comparison of uptake efficiencies of eight predicted peptides with HIV-1 TAT(48–60). As shown in Fig. 2, a significant intracellular FITC fluorescence intensity was detected for all the peptides except P2, suggesting that these peptides were internalized into HeLa cells. Of these peptides, P8 has shown the highest uptake and was internalized approximately 10 times ($p < 0.001$) more efficiently than TAT. On the other hand, P2 has shown the least uptake, whereas uptake of P1, P4 and P7 was comparable to TAT. Uptake of peptides P3 and P6 was significantly higher ($p < 0.05$) than TAT but lower than P8. Taken together these results suggest that seven out of eight peptides were internalized in HeLa cells with varying efficiencies.

3.3. Intracellular localization of peptides

To further confirm the FACS results, and for the visualization of internalized peptides, CLSM studies were performed. Results of CLSM are shown in Fig. 3. Live cell imaging by confocal microscopy showed that all peptides (P1, P3, P4, P5, P6, P7 and P8) except P2 were inside the HeLa cells. As seen in Fig. 3, in case of P1, P3, P4, P5, P6 and P7, a punctate cytoplasmic fluorescence was observed whereas P8 has shown both punctate and diffuse cytoplasmic fluorescence pattern. In contrast to above observations, HeLa cells treated with P2, have demonstrated an entirely different extracellular distribution, indicating a paracellular accumulation of the fluorescence suggesting that P2 could bind to the cell surface but did not internalize into the cells. This observation was consistent with the FACS data, where negligible P2 uptake was observed.

3.4. Sequence and structural analysis of peptides

In order to understand, why all examined peptides have shown different uptake efficiencies despite the presence of similar charge and an equal number of arginine residues, analysis of amino acid compositions and predicted structures of these peptides was carried out. It can be seen that peptide P4, P6 and P8 contain 2, 1, and 2 tryptophan residues, respectively (Table 3). Due to its aromaticity, tryptophan has been shown to have a strong preference for interactions at the membrane interface [34]. Many previous studies have highlighted the role of tryptophan in mediating internalization of peptides [35,36] and for few CPPs, the presence of tryptophan has been found to be indispensable for their internalization properties [37,38]. Thus, the presence of tryptophan in P4, P6 and P8 appears to be a predominant factor contributing to the superior internalization efficiencies of these peptides over the other peptides having no tryptophan residue.

It has been suggested that structure of peptides may play an important role in membrane interaction and insertion [39]. Several CPPs display a pronounced flexibility with a strong tendency to adopt helical structure in membrane mimicking environment, and it was proved that this helical structure plays a crucial role for their penetrating abilities [39]. Peptides with helical structure have been suggested to internalize more efficiently than the CPPs having random coil structures [39]. Since peptides P2, P5 and P7 contain proline residues (Table 3), which are known to destabilize the helix [40] and have lowest helix propensity [41], we next analyze, whether there is any correlation between the helical content and internalization of these peptides. To address this, we have predicted the 3D-structures of all these peptides using PEP-FOLD [27], which is a well-known *in silico* tool used for prediction of 3D structures of small peptides. The predicted structures of all peptides are shown in Fig. 4A. As demonstrated in Fig. 4A, peptides P3, P4, P6, and P8 have well defined helix conformation, whereas peptides P1, P2, P5, and P7 have almost random coil structures, which could be due to the presence of proline in these peptides. In order to obtain percent helical content in these peptides, we have assigned secondary structure states of each amino acid using DSSP program [28], which is a standard *in silico* algorithm for assigning secondary structure to amino acids of a protein. The helical content of peptides is shown in Table 3. We observed a decent correlation between the helical content and uptake efficiencies for most of the peptides. For instance, P6 and P8 have more than 70% helical content and have shown relatively higher uptake efficiencies. On the other hand, peptides P2 and P5 have minimum helical content (21.42% and 28.57%, respectively) and their uptake efficiencies were also very low. Taken together the results of primary and secondary structure analysis, it can be concluded that the relatively higher uptake efficiencies of P6 and P8 could be due to the presence of tryptophan and the tendency of these peptides to adopt

Table 2
Name, sequence and source of peptides selected for experimental validation.

Designation	Sequence	Region (aa)	SwissProt ID	Protein name	Organism
P1	KKKKKKNKKLQQRGD	87–101	Q9SB89	DEAD-box ATP-dependent RNA helicase 27	*Arabidopsis thaliana*
P2	RGDGPRRRPRKRRGR	431–445	Q63003	5E5 antigen	RAT
P3	RRRQKRIVVRRRLIR	497–511	Q01351	Protein U4	Human herpesvirus
P4	RRVWRRYRRQRWCRR	881–895	P56877	PE-PGRS3	*Mycobacterium tuberculosis*
P5	RRARRPRRLRPAPGR	501–515	P17471	Envelope glycoprotein B	Bovine herpesvirus
P6	LLRARWRRRRSRRFR	231–245	P35375	Prostaglandin E2 receptor EP1 subtype	Mouse
P7	RGPRRQPRRHRRPRR	356–370	Q9UN88	GABA receptor subunit theta	Human
P8	RRWRRWNRFNRRRCR	503–517	Q01668	Voltage-dependent L-type calcium channel subunit alpha-1D	Human

Table 3
Amino acid composition, charge, and CellPPD prediction scores of all examined peptides.

Name	Arginine	Tryptophan	Proline	Charge	CellPPD score[a]	Helicity (%)[b]
P1	1	0	0	+9	0.35	28.57
P2	8	0	2	+8	1.01	21.42
P3	8	0	0	+9	0.56	64.20
P4	9	2	0	+9	0.92	64.20
P5	8	0	3	+8	0.92	28.57
P6	9	1	0	+9	1.26	78.57
P7	9	0	3	+9.5	1.03	35.71
P8	9	2	0	+9	0.76	71.40

[a] CellPPD is an *in silico* algorithm developed for the prediction of cell penetrating potential of peptides. It provides a CellPPD score (SVM score) to each submitted peptide. Higher the score, higher will be the possibility of a peptide to be CPP.
[b] Percent helicity of peptides was calculated from the secondary structure states of peptides, which have been assigned from predicted tertiary structures using software DSSP.

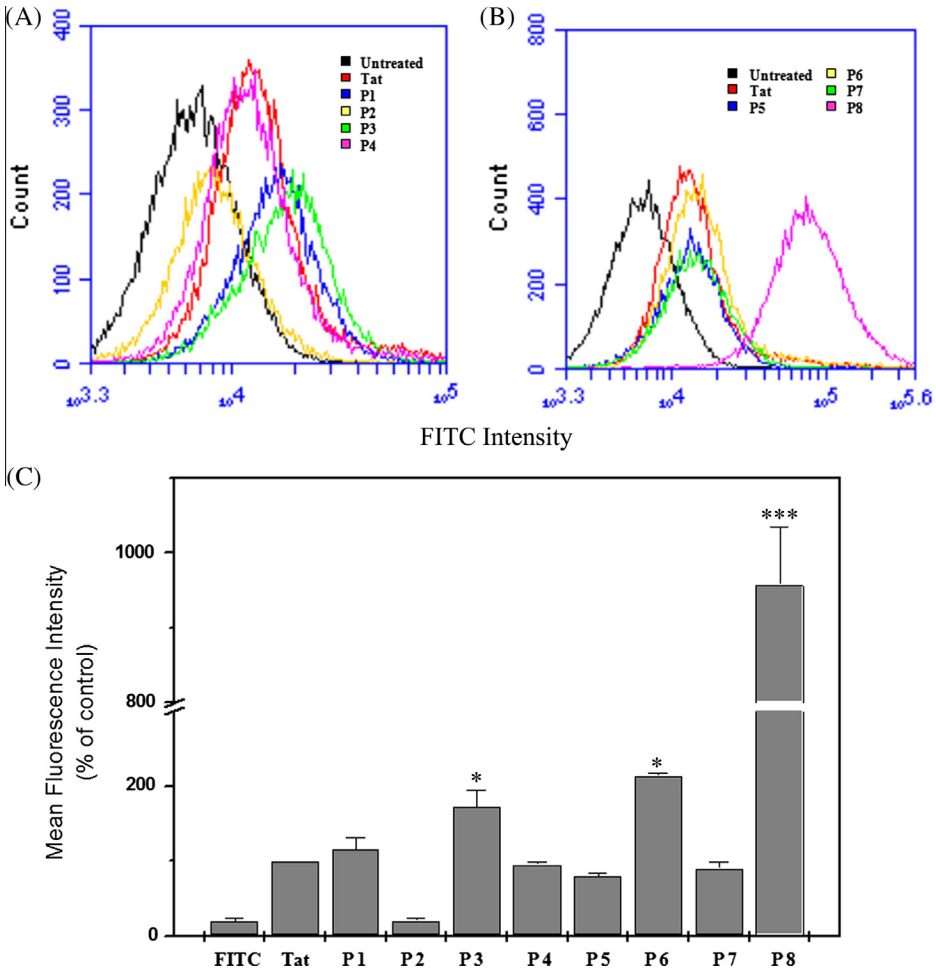

Fig. 2. Cellular uptake of FITC-labeled peptides as determined by FACS analysis. Frequency distributions of FITC fluorescence intensity in HeLa cells incubated with FITC-labeled peptides (A) P1, P2, P3 & P4 and (B) P5, P6, P7, & P8. Overnight grown HeLa cells were incubated with 10 μM FITC-labeled peptides for 1 h in complete medium. After the incubation, cells were washed with PBS, rinsed with heparin (100 μg/ml), and then treated with trypsin (1 mg/ml) at 37 °C for 10 min. Finally cells were suspended in PBS, and subjected to flow cytometry. (C) Bar diagram showing the uptake of FITC-labeled peptides as mean cellular fluorescence from the flow cytometric analysis of all live cells positive for FITC. The fluorescence of cells treated with TAT peptide was set to 100% and relative uptake of all peptides (P1–P8) was plotted as percentage of control. Results are expressed as mean ± S.E., based on triplicates of at least two independent experiments. Asterisks indicate significance according to student's *t*-test (two-tailed); ($^{*}p < 0.05$, $^{***}p < 0.001$).

helical structures. However, future experimental studies would shed more light on this.

Interestingly, it has been observed that both P4 and P8 are quite similar in terms of their sequence and structure. Both peptides have almost similar helical content (64% and 71% respectively) and have two tryptophan residues. Despite these similarities, their uptake efficiencies are significantly different. It has been shown recently that apart from the number of tryptophan; backbone spacing of tryptophan in the peptide sequence also affects the internalization efficacies [36]. The order of tryptophan residues in both peptides is different. In P8, both tryptophan residues are in proximity and are at N-terminus while, in P4, both residues are placed at distal ends (Table 3). Therefore, we next wanted to examine the differences in the orientation of arginine and

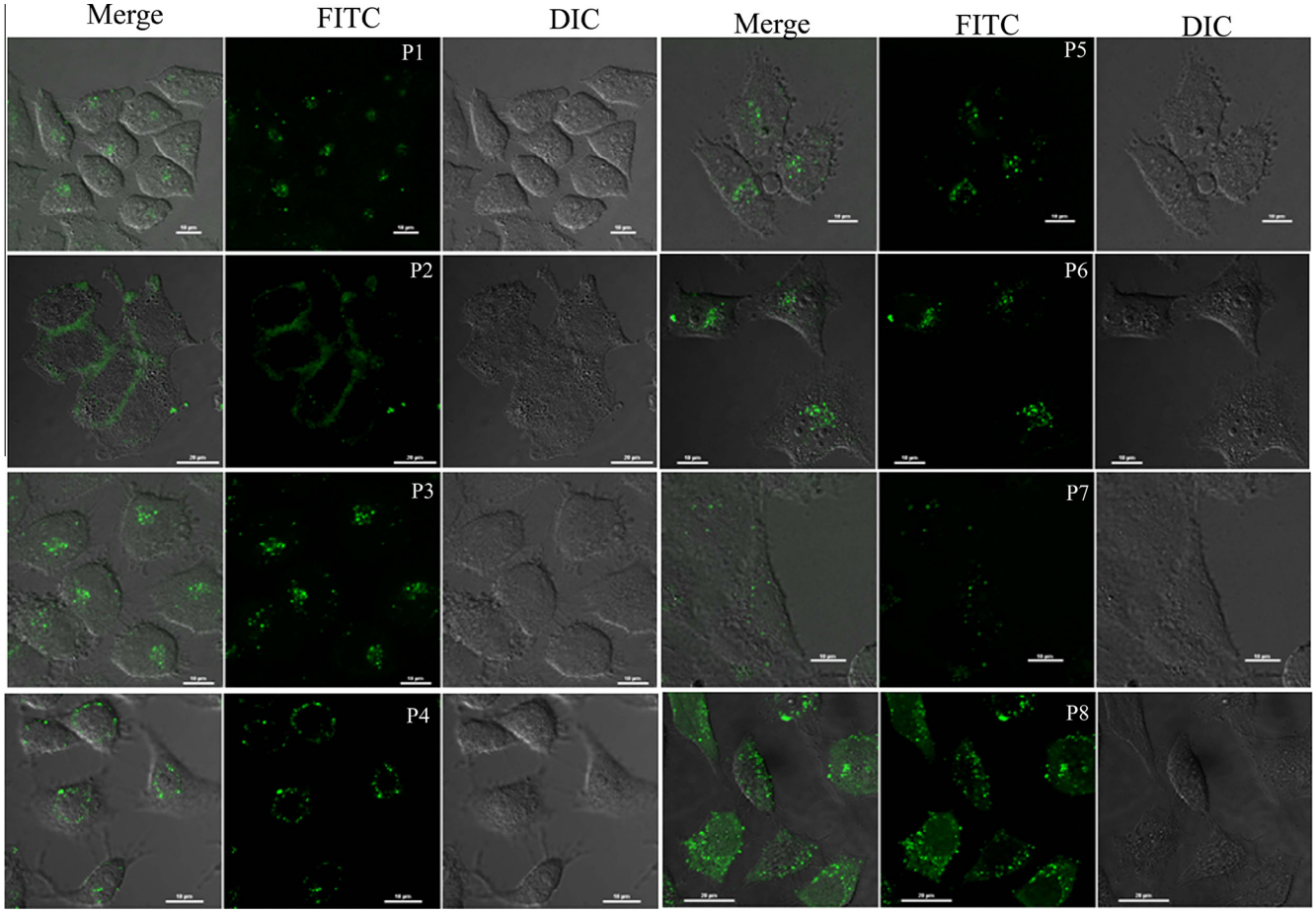

Fig. 3. Intercellular localization of FITC-labeled peptides in HeLa cells. HeLa cells were grown on coverslips and incubated with FITC-labeled peptides (10 μM) at 37 °C in complete medium for 1 h. Cells were then washed with PBS and immediately observed (without fixation) by confocal fluorescence microscopy. Bar = 10 μm. The laser intensity and photomultiplier settings have been adjusted to get the best images therefore, the intensities are not directly comparable.

tryptophan side chains, if any, between P4 and P8. It was also observed that, for many known CPPs, their cationic amino acids existed in one side on the wheel from helical wheel projection analysis. So, we have generated helical wheel structures of these peptides. As shown in Fig. 4B, a significant difference in the distribution of tryptophan and arginine residues between P4 and P8 was observed. In P8, most of the arginine (7 arginine) residues are clustered together on one phase of helix, and both tryptophan residues are clustered at the opposite phase of the helix similar to an amphipathic helical distribution, whereas, in P6 arginine residues are not clustered together and distributed throughout of the helix. In addition, tryptophan residues are not present at the opposite phase of the helix rather they are placed in between the arginine showing an entirely different distribution than P8 (Fig. 4B). A similar difference in the distribution of arginine and tryptophan was also reported for RWmix and W4R8 peptides, which has suggested to be associated with high uptake efficiency of RWmix than W4R8 [36]. Therefore, it gives a clue that these differences in the orientation of arginine and tryptophan residues between P4 and P8 might be responsible for significant differences in their internalization and uptake efficiencies.

3.5. Cytotoxicity of peptides

For an ideal drug delivery system, high cell-penetrating properties must be combined with low cytotoxicity. Therefore, toxicities of all predicted peptides were examined on HeLa cells by incubating HeLa cells with increasing concentrations (5, 10, 20, 40 and 80 μM) of unlabeled peptides for 24 h. Toxicity profiles of these peptides on HeLa cells are shown in Fig. 5. As shown, none of the peptides showed significant cytotoxicity up to 80 μM concentration, which is much greater concentration than normally used (5 μM). Approximately more than 85% cells are viable up to 80 μM concentration. However, only in case of P8, 25% decrease in cell viability was observed at 80 μM.

3.6. Characterization of P8

As shown in Figs. 2 and 3, among all eight peptides, P8 has shown the highest internalization into live cells; therefore, we selected P8 for further characterization.

3.6.1. P8 internalize in a variety of cells and uptake of P8 is very rapid and concentration-dependent

Peptide P8 is a 15-amino acid peptide (503–517 aa), derived from a cytoplasmic domain of human voltage-dependent L-type calcium channel subunit alpha-1D (Fig. 6A). First, in order to ascertain the versatility of P8, we analyzed the uptake of P8 in various cell lines (HeLa, PC-3, RWPE-1, and CHO-K1 cells). As shown in Fig. 6B, P8 internalized in all cell lines suggesting that uptake was not cell type specific and thus P8 could be a versatile vector. Next, to assess the uptake properties of P8, the concentration dependent and time-course study of P8 internalization in HeLa cells was investigated. For this, HeLa cells were incubated with

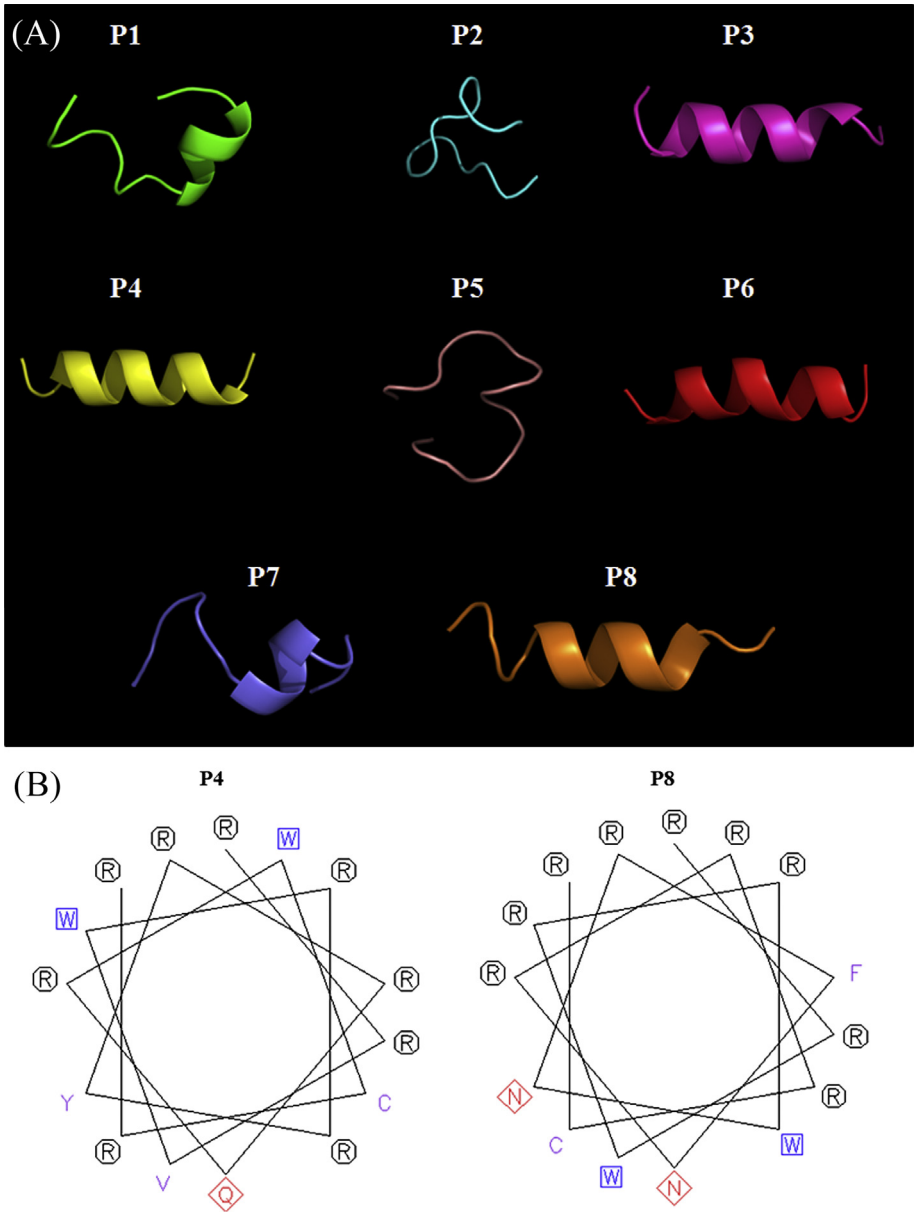

Fig. 4. Structural analysis of peptides. (A) Tertiary structures of all peptides examined were predicted using PEP-FOLD. The figures were generated with PyMol (W.L. DeLano, The PyMol Molecular graphics system (2002) http://www.pymol.org). (B) Helix wheel projections were generated using PEPwheel tool of emboss.

P8 (10 μM) for different time periods (5, 20, 30 and 60 min) followed by flow cytometry analysis. Fig. 6C and D demonstrates the time-dependent internalization of P8 into HeLa cells. Result revealed that uptake of P8 was rapid and very efficient. Uptake of P8 was started immediately upon its addition to cells and reached equilibrium after as early as 10 min incubation (Fig. 6D). Even after 5 min, P8 entered in approximately 90% of the cells (Fig. 6D).

In order to further assess the extent of peptide internalization, flow cytometry analysis of HeLa cells exposed for 30 min to increasing concentrations (0, 2.5, 5, 10 and 20 μM) of FITC-labeled P8 was performed. Flow cytometry analysis revealed that the FITC fluorescence intensity was markedly increased with peptide concentration, suggesting that the amount of internalized P8 by cells increased with peptide dose, within the concentration range examined (Fig. 6E). These results suggest that P8 is a versatile CPP, which can enter into live cells very efficiently in a dose- and time-dependent manner. Further, in order to examine the conformation of P8 in membrane mimicking environments *i.e.* 90% 2,2,2-trifluoroethanol (TFE) and SDS micelles, we have carried out CD spectroscopy and analyzed the CD spectra of P8 in water and membrane mimicking environments. Unlike TAT, P8 adopted helical conformation in both 90% TFE and SDS micellar environments (Supplementary Fig. S1).

To examine the effect of serum on the uptake of P8, HeLa cells were incubated with FITC-labeled P8 in the presence and absence of serum for 30 min. Presence of 10% serum decreased the P8 uptake by approximately 3-fold (Fig. 6F). This retardation in P8 uptake could be due to non-specific electrostatic interaction of P8 with serum proteins. This interaction of P8 with serum proteins was further confirmed by HPLC (data not shown).

3.6.2. Peptide 8 internalize by a temperature-sensitive and energy-dependent process

The internalization of CPPs into live cells has been occurred mainly via two routes: (i) by direct translocation and (ii) by

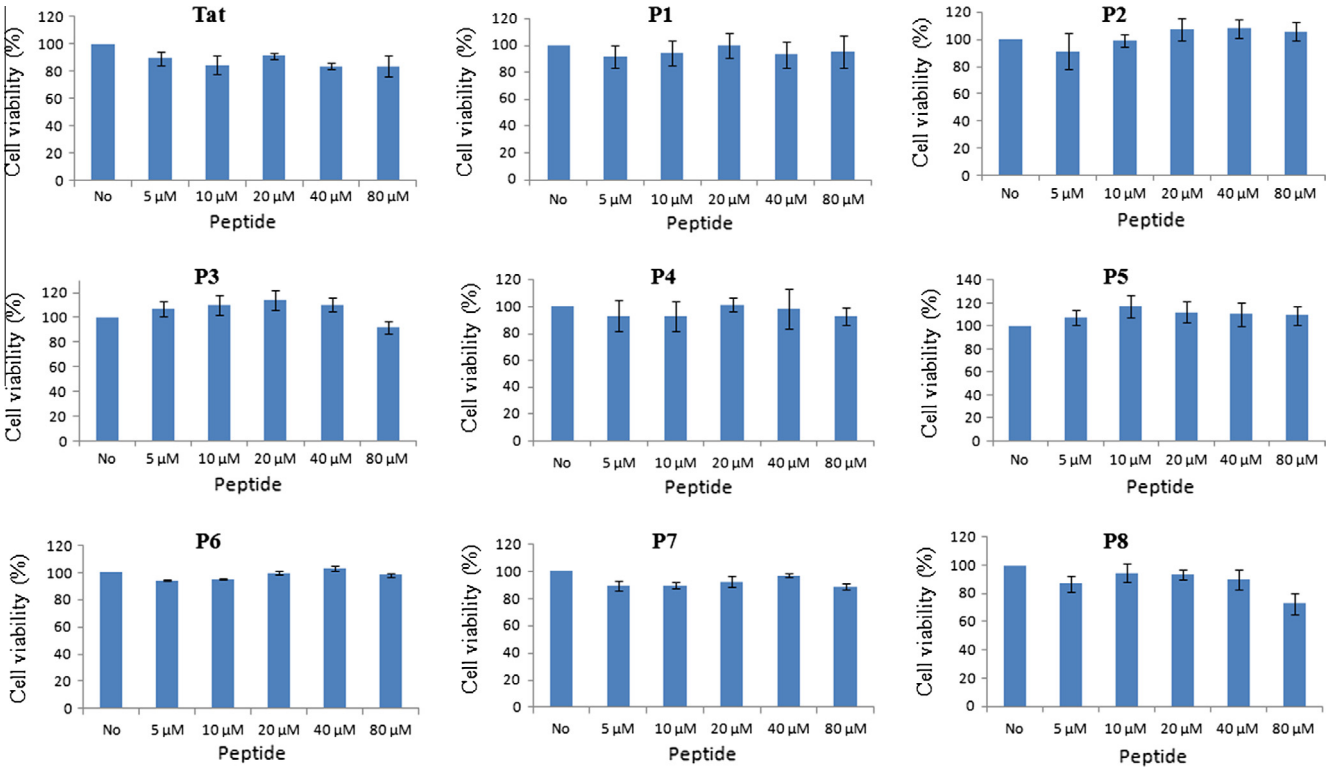

Fig. 5. Cytotoxicity of peptides. HeLa cells were incubated with increasing concentrations (0, 5, 10, 20, 40 and 80 μM) of peptides in serum containing medium at 37 °C for 24 h. Cell viability was measured by MTS assay. Viability of control (without peptide) was taken as 100% and viabilities of cells treated with increasing concentration of peptides were plotted as percentage of control. Results are expressed as mean ± S.E, based on triplicates of at least two independent experiments. (For interpretation of the references to color in this figure legend, the reader is referred to the web version of this article.)

endocytosis [24]. In order to characterize the internalization route used by P8 peptide, its uptake was performed at low temperature (4 °C). Since endocytosis is an energy-governed process, incubation of cells at low temperature is expected to block all the endocytic processes but not block the entry by direct translocation, which is an energy independent process. Therefore, internalization experiments were performed at low temperature by incubating HeLa cells at 4 °C in Opti-MEM and uptake of P8 was analyzed by both flow cytometry and CLSM. As shown in Fig. 7A and B, a significant decrease (up to 80%, $P < 0.05$) in P8 uptake was observed when incubated at 4 °C as compared to 37 °C. Similar results were obtained in CHO-K1 cells (data not shown). Few reports have proposed that the lack of internalization at 4 °C could be due to increased membrane rigidity at low temperatures [42]. Therefore, to further confirm that lack of P8 internalization is not because of high membrane rigidity, HeLa cells were treated for 30 min with 0.1% sodium azide and 50 mM DOG to deplete the intracellular ATP levels followed by incubation with FITC-labeled P8 for 30 min at 37 °C. As shown in Fig. 7A and B, ATP depletion significantly inhibited P8 uptake by 50% ($p < 0.05$). These results were consistent with the confocal microscopy observations where no significant FITC fluorescence was observed in HeLa cells after incubation at 4 °C as well as after ATP depletion (Fig. 7C). In light of these findings, it can be speculated that major fraction of P8 internalized by a temperature-sensitive and energy-dependent process, which could be endocytosis.

Since lysosomes are known to be the final destination of molecules, which enter the cell through endocytosis, therefore to confirm whether P8 enters HeLa cells through endocytic pathway, the localization of FITC-labeled P8 and lysosomes was compared. As shown in Fig. 7D, a major fraction of FITC-labeled P8 co-localized with LysoTracker Red dye, which specifically binds to late endosomes/lysosomes suggesting that P8 is present in these compartments under testing conditions. Thus, these results provide evidence that P8 internalized in HeLa cells through endocytosis.

3.6.3. Peptide 8 internalized by heparan sulfate proteoglycan-mediated macropinocytosis

Given the results demonstrating that P8 internalized by endocytosis, we next wanted to explore the specific endocytic pathway involved in P8 uptake. First, in order to determine the involvement of heparan sulfate proteoglycans in the internalization of P8, its uptake was analyzed in the presence of heparin, which mimics the glycosaminoglycans (GAGs) moieties of proteoglycan present at the cell surface. As shown in Fig. 8A, the presence of heparin blocked the P8 uptake significantly (90%, $p < 0.01$) suggesting the involvement of GAGs in the P8 uptake.

Endocytic processes can be grouped into two broad categories: phagocytosis and pinocytosis [43]. Phagocytosis is a phenomenon, which occurs in certain specialized cells, whereas pinocytosis occurs in most of the cell types. Pinocytosis is further classified into three main categories: (i) clathrin-dependent endocytosis, (ii) clathrin-independent endocytosis, and (iii) macropinocytosis. In order to investigate the possible involvement of the different endocytic pathways in the internalization of P8, effect of various inhibitors, which block the endocytic pathways, was examined on P8 uptake. For this, chlorpromazine (CPZ), a known inhibitor of clathrin-mediated endocytosis [44], MβCD, an inhibitor of the lipid raft mediated endocytosis [45], amiloride, an inhibitor of Na^+/H^+ exchange required for macropinocytosis, and cytochalasin D (CytD), an inhibitor of F-actin elongation required for macropinocytosis, were used. Fig. 8A and B shows the effect of these drugs on P8 uptake in HeLa cells. Results demonstrate that both CPZ and MβCD were unable to block the P8 uptake. Interestingly, we observed an increase, rather than a decrease, in the cellular uptake

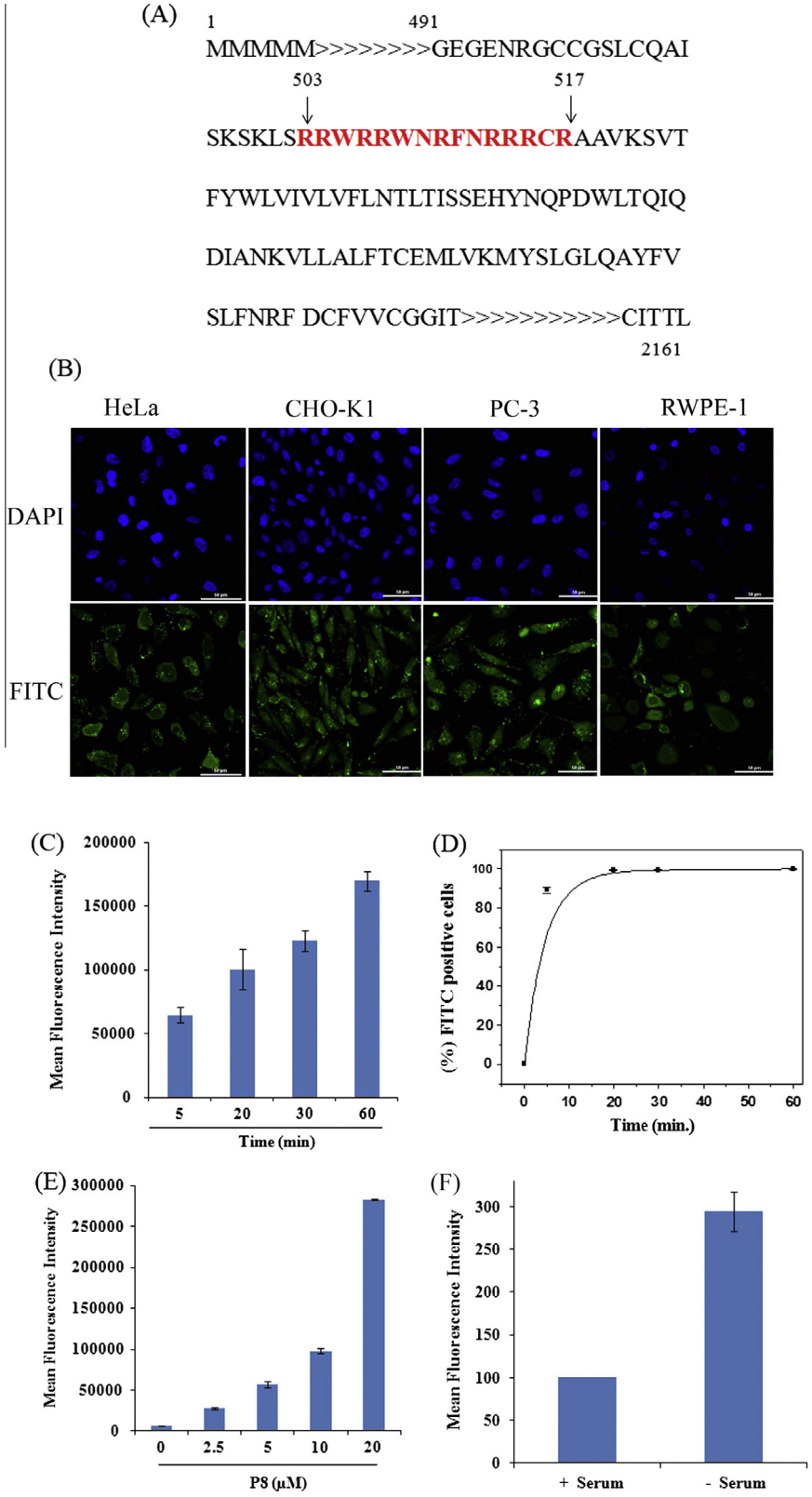

Fig. 6. Characterization of P8. (A) Protein sequence of human voltage-dependent L-type calcium channel subunit alpha-1D. P8 sequence (15 amino acids, 503–517) is highlighted. (B) Confocal images of various live cells (HeLa, CHO-K1, PC-3 and RWPE-1) showing internalized P8. (C) and (D) Time dependent uptake of P8. HeLa cells were incubated with 10 μM FITC-labeled P8 for increasing time periods (0, 5, 20, 30 and 60 min) followed by trypsinization (1 mg/ml, 10 min) and flow cytometry quantification of peptide uptake. (E) Concentration dependent internalization of P8 peptides. HeLa cells were incubated with increasing concentration (0, 2.5, 5, 10, 20 μM) of FITC-labeled P8 for 30 min followed by trypsinization and flow cytometry quantification of peptide uptake. (F) Effect of serum on P8 uptake. HeLa cells were treated with 10 μM FITC-labeled P8 peptide with and without serum containing medium for 30 min followed by flow cytometry analysis. Uptake of P8 in the presence of serum was set to 100% and uptake of P8 in the absence of serum was plotted as percentage of control. Data are shown as mean ± S.E, based on triplicates of at least two independent experiments.

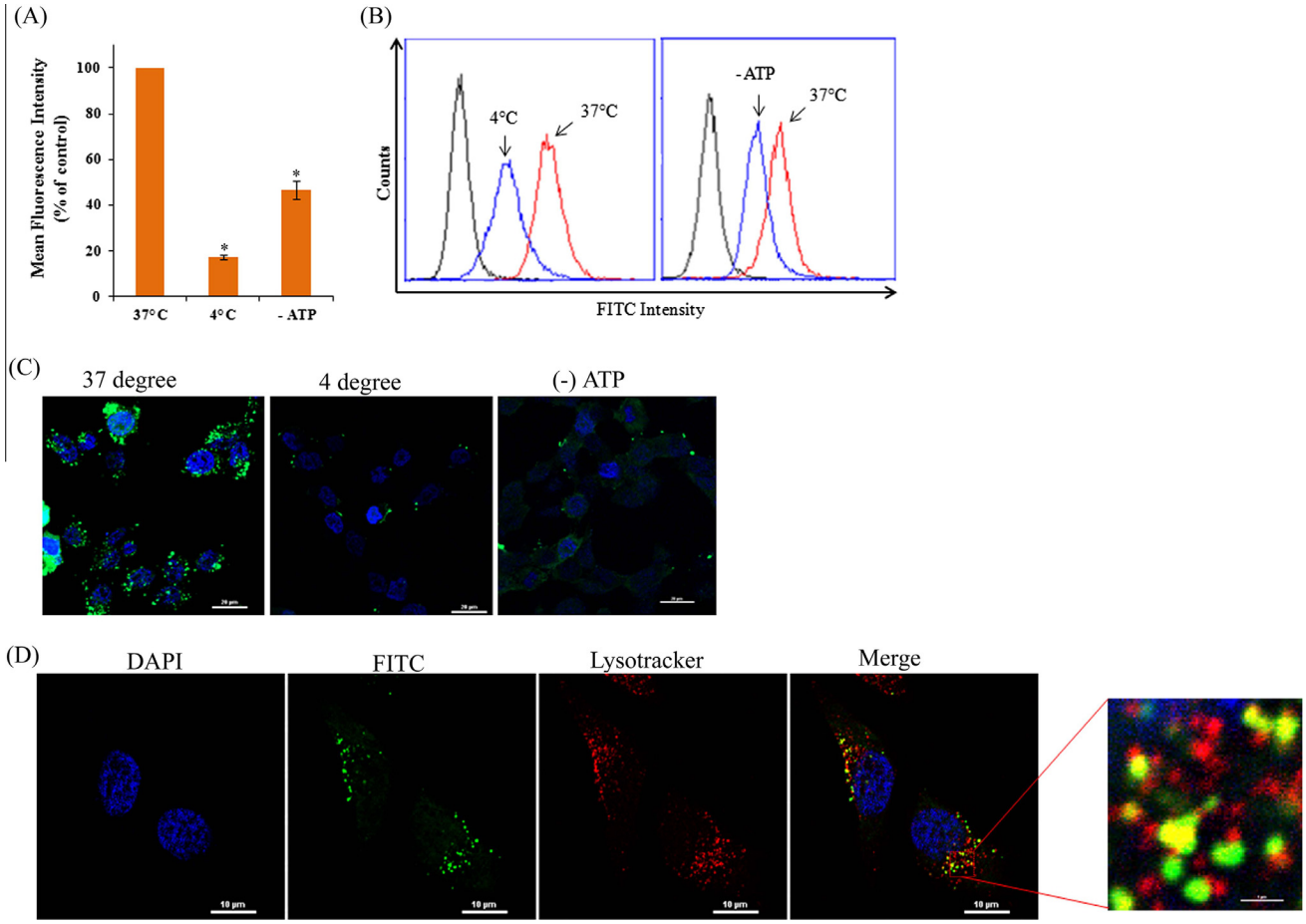

Fig. 7. Effect of low temperature and energy depletion on the uptake of P8 peptide. (A) and (B) Flow cytometry, and (C) confocal microscopic analysis of cellular uptake of P8 at low temperature and at ATP depleted conditions. HeLa cells were either pre-incubated at 4 °C or pre-treated with energy-depletion medium for 30 min, and then incubated with 5 μM peptide for 30 min under the same conditions, as described in the methodology. Uptake of P8 at 37 °C was set to 100% and relative uptake of P8 at 4 °C and in energy-depletion condition was plotted as percentage of control. Confocal microscopic analysis was performed in live cells. In (A), data are shown as means ± S.E, based on triplicates of at least two independent experiments. Asterisks indicate significance according to student's *t*-test (two-tailed); (*$p < 0.05$). (D) Confocal images showing co-localization between FITC-labeled P8 and LysoTracker Red. Overnight grown HeLa cells were incubated both with FITC-P8 (5 μM) and LysoTracker Red (100 nM) for 30 min at 37 °C. Cells were washed with PBS (3×) and live cells were imaged. Scale bars are 10 μm.

efficiency of P8 after treatment with CPZ, and MβCD, suggesting that uptake of P8 might be enhanced by some compensatory mechanism when blocking individual pathway as it has been shown to be the case in previous reports [46,47]. However, a significant decrease (40%, and 60%, $p < 0.05$) in P8 uptake was observed when treated with CytD and amiloride (Fig. 8A and B) suggesting that peptide 8 is using macropinocytosis for internalization in HeLa cells. To further visualize the macropinocytic uptake of P8, dextran (70 kDa) labeled with tetramethylrhodamine was added to cells along with FITC-labeled P8 and their localization was compared. Confocal microscopic examination demonstrated co-localization of FITC-labeled P8 with TMR-dextran as shown in Fig. 8C. Based on these results, it can be concluded that macropinocytosis seems to be the major route of P8 entry under the testing conditions.

4. Discussion

The aim of the present study was to identify novel natural protein-derived efficient CPPs. For this purpose, we have applied an *in silico* procedure to identify putative CPP candidates in the proteins available in SwissProt database. Since the optimum number of arginine residues required for the high cellular uptake is between 7 and 10, we have extracted peptides having 8/9 arginine in all the proteins available in SwissProt database using *in silico* approach. A window size of 15 amino acids was chosen because most of the CPPs have an average length between 10 and 18 amino acids [14] and CPP having a length of 15 amino acids are easy and cost-effective to synthesize. In addition, longer peptides cannot escape the presentation by MHC-II, which prefers peptides between 15 and 24 residues in length [48].

The extracted peptides were further subjected to various filters to find out the potential CPP sequences. CPPs are not cell specific and thus are internalized in receptor independent manner in almost all cell types. Therefore, to identify CPPs, which can be cancer specific or can penetrate cancer cells effectively, peptides having the tumor homing motif RGD and/or tumor penetrating motif (RXXR motif) were also selected with an expectation that such peptides would have both cell penetrating and tumor homing properties. It has been shown that peptides with RXXR motif at C-terminus are internalized in tumor cells by binding to neuropilin receptor, often expressed at the surface of tumor cells. Therefore, peptides with and without these motifs were screened and extracted. To achieve a higher success rate, the cell-penetrating potential of all screened peptides was predicted using a computational algorithm, CellPPD [25], which is a support vector machine-based prediction method developed to predict highly efficient CPPs. CellPPD method is based on binary profile of peptides, which

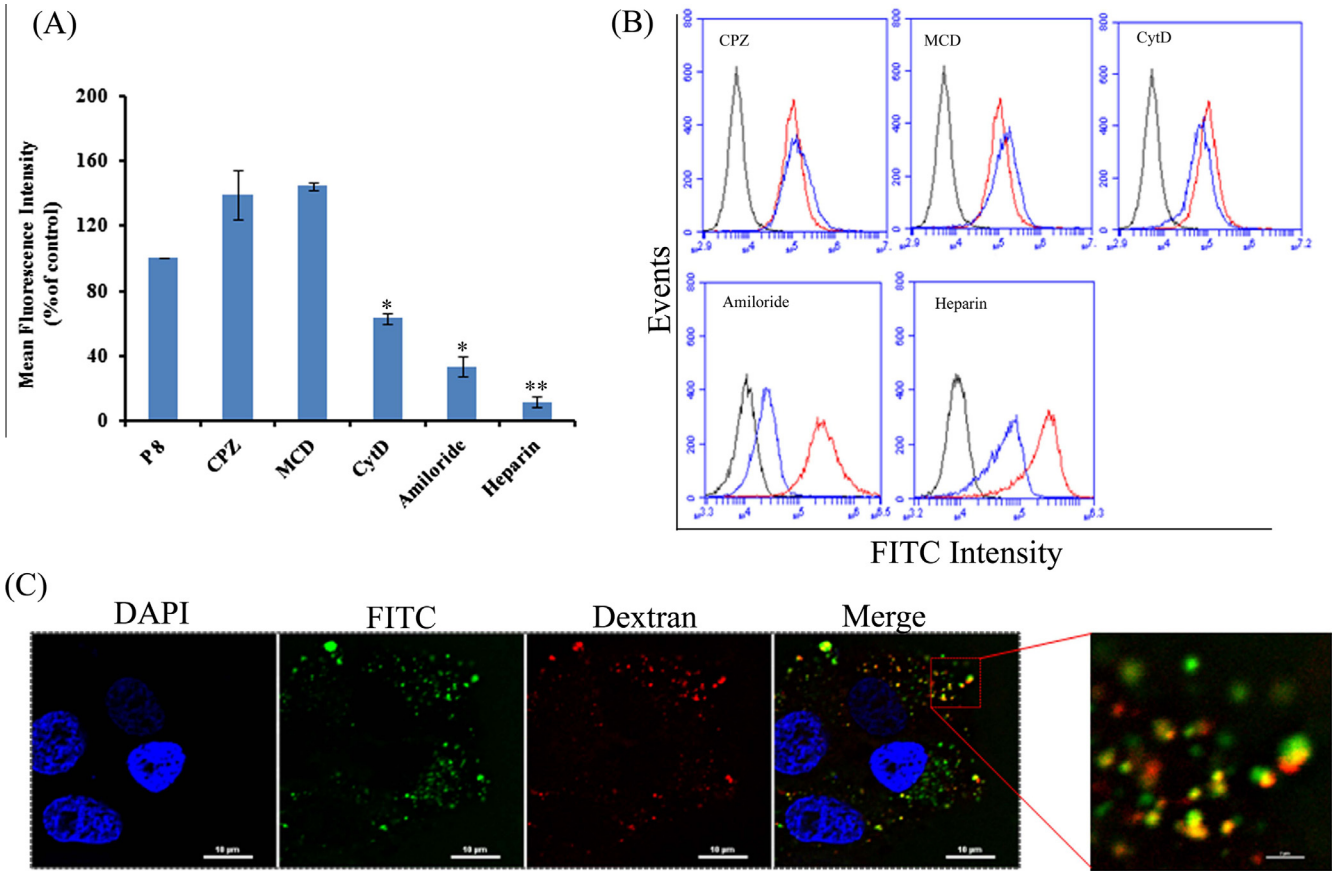

Fig. 8. Effect of endocytosis inhibitors on uptake of P8. Cellular uptake of P8 (A and B) by HeLa cells in the presence of endocytic inhibitors were determined by flow cytometry. HeLa cells, pre-treated with CPZ (30 μM), MβCD (5 mM), CytD (10 μM), amiloride (5 mM) and heparin (10 μg/ml) for 30 min at 37 °C, were incubated in the presence of FITC-labeled P8 (5 μM) at 37 °C for additional 30 min. Following this, cells were trypsinized for 10 min, washed twice with PBS, and subjected to flow cytometry. The uptake is measured as mean cellular fluorescence from the flow cytometric analysis of all live cells positive for FITC. The uptake of P8 in the absence of any inhibitor was set as 100% and relative uptake of P8 in the presence of inhibitors was shown as percentage of control. (B) Frequency distributions of FITC fluorescence intensity in HeLa cells incubated for 30 min with (blue line) and without (red line) indicated endocytic inhibitors. Black color histograms stand for untreated cells (control). Data are shown as mean ± S.E, based on triplicates of at least two independent experiments. Asterisks indicate significance according to student's *t*-test (two-tailed); (*$p < 0.05$; **$p < 0.01$). (C) Confocal images of HeLa cells showing co-localization between FITC-labeled P8 and tetramethylrhodamine conjugated dextran-70 kDa. Overnight grown HeLa cells were incubated simultaneously with FITC-P8 (5 μM) and tetramethylrhodamine conjugated dextran-70 kDa (200 μg/ml) for 30 min at 37 °C. Cells were washed with PBS and live cells were imaged.

incorporates the information of both order and composition of amino acids in peptides.

FACS and CLSM results revealed that seven out of eight peptides have cell penetrating properties. Interestingly, none of the peptides showed significant membrane toxicities even at 80 μM concentrations suggesting that these peptides could be used for future drug delivery applications. We also determined the toxicities of these peptides on CHO-K1 and HepG2 cells, and no significant toxicity was observed in these cells by any of the peptides at all the concentrations tested except P8, which showed some toxicities at higher concentrations (data not shown).

All peptides displayed cell-penetrating potential except one peptide, P2, which did not internalize into the cells rather it could bind to the cell surface as most of the fluorescence was observed at the periphery of the cells, when observed under confocal microscope. Peptide P2 has RGD at N-terminus and RGD motif has been shown to selectively recognize and bind αvβ3 and αvβ5 integrins that are expressed on cell surfaces of various cancer cell types, including HeLa cells [49,50]. The lower uptake of P2 could be due to binding of peptide with integrins on HeLa cells. Therefore, it would be interesting to evaluate the uptake of P2 on other non-cancerous cell types. The focus of the present study was to determine the cell-penetrating potential of predicted peptides, therefore the role of RGD and RXXR motif has not been explored in the present study. Subsequent research will focus on exploring the role of both motifs present in these peptides in terms of cancer specificity and their internalization.

In general, CPPs having equal charge and arginine content are expected to have equal uptake efficiencies. However, in the present study, even though all peptides have almost similar arginine content and overall charge, they displayed different uptake efficiencies. For example, there is a drastic difference in uptake efficiencies between P8 and other peptides. However, our results are in agreement with a previous study by Nakase et al., where they have observed that arginine-rich peptides with similar charge and arginine content internalized into HeLa cells with different efficiencies [51]. Due to the presence of guanidinium groups, which interact with negatively charged components of membrane, arginine residues have been suggested to play a more crucial role in CPP internalization than lysine/histidine residues [52,53]. Surprisingly, P1, which is a lysine-rich peptide, showed approximately 10 times higher uptake than P2, which is an arginine-rich peptide (Fig. 2). Taken together from these results, it can be concluded that the number of arginine residues is not the only factor associated with high internalization of arginine-rich CPPs and other factors may also contribute in the internalization and uptake efficiency. *In silico* analysis aimed at identifying features responsible for varying efficiencies of these arginine-rich peptides points to the

presence of other amino acids such as tryptophan and tendency to adopt helical structures. Orientation of arginine and tryptophan residues around the helix might also be responsible for differences in the uptake efficiencies. These observations are consistent with the previous findings where the presence of tryptophan and spacing of arginine residues have been found to affect the uptake efficiency of CPPs [36].

Further characterization then focused on the P8 peptide, which showed almost 10 times higher uptake in HeLa cells than TAT. The uptake of P8 was also observed in other cell types, including CHO-K1, THP-1, MCF-7 and NCI-H522 (data not shown) suggesting that uptake of P8 is not cell type specific and it can be used as an efficient delivery system. P8 is derived from a cytosolic domain of human voltage-dependent L-type calcium channel subunit alpha-1D protein and contains 2 tryptophan and 8 arginine residues. *In silico* analysis as well as CD analysis (Supplementary Fig. S1) in membrane mimicking environments revealed that P8 has a tendency to form helical structure. Helical wheel analysis of P8 demonstrates the partially amphipathic distribution of arginine and tryptophan residues. It has been shown previously that helical peptides are internalized more effectively than the peptides with random coil structures [39]. Therefore, the presence of tryptophan and tendency to adopt amphipathic helical conformation might help to explain the superior uptake of P8 in live cells. Despite its higher uptake efficiency, P8 did not show any significant membrane toxicity up to 40 μM concentration, which is much higher than the routinely tested concentrations. However, at 80 μM concentration, it showed some toxicity as only 75% HeLa cells were viable at this concentration. Our explanation for this toxicity might be that, at higher concentration, it causes holes in the cell membranes. High penetrating efficiency with low toxicity makes P8 an ideal candidate for drug delivery vehicle. However, presence of serum retards its uptake efficiency by ~3-fold, suggesting that P8, being a highly cationic peptide, might interact non-specifically with serum proteins. Such effects of serum on uptake efficiency have also been reported for other CPPs [19]. This inhibition of uptake efficiency by serum proteins is sometimes beneficial, particularly when the CPP is highly effective such as P8; otherwise this high uptake may cause cytotoxicity.

Taking into consideration that the internalization of P8 occurs by a temperature-sensitive and energy-dependent process, the involvement of specific endocytosis pathway was thoroughly investigated by analyzing P8 uptake in the presence of drugs that selectively inhibit different endocytic pathways. Two inhibitors CPZ and MβCD, which are known to block clathrin-mediated endocytosis and lipid-raft mediated endocytosis respectively, were unable to block the cell entry of P8 (Fig. 8), therefore ruling out the contribution of these two entry pathways in P8 internalization. However, CytD and amiloride, which are inhibitors of macropinocytosis, were capable of attenuating the cell-penetrating activity of FITC-labeled P8 and thus providing evidence for the involvement of macropinocytosis as a major entry mechanism. In addition, co-localization of P8 with dextran (a marker of macropinocytosis) further supported the previous finding.

The first step in the internalization of most of the cationic CPPs has been suggested to be the interaction of these CPPs with negative components of plasma membrane *e.g.*, proteoglycans [54,55]. Membrane-associated proteoglycans have been reported to be involved in the induction of F-actin organization and macropinocytosis [56]. This prompted us to further seek the involvement of GAGs in P8 internalization. In line with the other CPPs, treatment with heparin, a mimic of GAGs, significantly blocked the entry of P8 suggesting that GAGs play an important role in P8 uptake. Therefore, the possible uptake mechanism could be that first, P8 interacts electrostatically with negatively charged GAGs present on cell surface followed by its internalization by macropinocytosis, which is a highly conserved endocytic pathway by which large volume of extracellular fluid is internalized into the cells. Altogether, these results suggest that P8 has potential to become a versatile delivery system. Although further studies are needed to assess the capability of P8 for delivering therapeutic molecules.

In summary, the present study provides strong evidence that integrated *in silico* and experimental approach could be a promising strategy to identify novel efficient CPPs, as it saves both time and money consumed in the initial wet laboratory screening of CPPs. In addition, we have identified a few novel CPPs, in particular, P8 which has shown efficient cell-penetrating ability with low toxicity. Thus, P8 could be a promising candidate for future applications as a vector for intracellular transport.

Author contribution

AG and GPSR conceived the study, designed and interpreted the experiments. AG, PV, MS and PK performed the experiments. AG and KC performed the *in silico* screening of peptides. RK, MS and SKN synthesized and purified the peptides. AG and GPSR wrote the paper.

Conflict of interest

The authors declare that they have no conflict of interests.

Acknowledgments

Authors are thankful to Mr. Deepak Bhatt and Ms. Anjali Koundal for their help with confocal experiments, Mr. Sudheer Gupta and Mr. Sandeep Dhanda for their efforts in establishing wet laboratory and Dr. Manoj Raje for critically reading and editing the manuscript. We are also thankful to Dr. Satya Prakash for helping in CD experiments. This work was supported by Council of Scientific and Industrial Research (Project OSDD and GENESIS BSC0121) and Department of Biotechnology (Project BTISNET), Govt. of India. A part of this study has been patented (Application No. 3380DEL2013).

Appendix A. Supplementary material

Supplementary data associated with this article can be found, in the online version, at http://dx.doi.org/10.1016/j.ejpb.2014.11.020.

References

[1] H. Margus, K. Padari, M. Pooga, Cell-penetrating peptides as versatile vehicles for oligonucleotide delivery, Mol. Ther. 20 (2012) 525–533.
[2] I. Nakase, G. Tanaka, S. Futaki, Cell-penetrating peptides (CPPs) as a vector for the delivery of siRNAs into cells, Mol. BioSyst. 9 (2013) 855–861.
[3] A. Presente, S.F. Dowdy, PTD/CPP peptide-mediated delivery of siRNAs, Curr. Pharm. Des. 19 (2012) 2943–2947.
[4] S. Trabulo, A.L. Cardoso, A.M. Cardoso, C.M. Morais, A.S. Jurado, M.C. de Lima, Cell-penetrating peptides as nucleic acid delivery systems: from biophysics to biological applications, Curr. Pharm. Des. 19 (2012) 2895–2923.
[5] N.Q. Shi, W. Gao, B. Xiang, X.R. Qi, Enhancing cellular uptake of activable cell-penetrating peptide-doxorubicin conjugate by enzymatic cleavage, Int. J. Nanomed. 7 (2012) 1613–1621.
[6] L. Walker, E. Perkins, F. Kratz, D. Raucher, Cell penetrating peptides fused to a thermally targeted biopolymer drug carrier improve the delivery and antitumor efficacy of an acid-sensitive doxorubicin derivative, Int. J. Pharm. 436 (2012) 825–832.
[7] S.A. Nasrollahi, S. Fouladdel, C. Taghibiglou, E. Azizi, E.S. Farboud, A peptide carrier for the delivery of elastin into fibroblast cells, Int. J. Dermatol. 51 (2012) 923–929.
[8] P. Boisguerin, J.M. Giorgi, S. Barrere-Lemaire, CPP-conjugated anti-apoptotic peptides as therapeutic tools of ischemia-reperfusion injuries, Curr. Pharm. Des. 19 (2012) 2970–2978.
[9] R.H. Mo, J.L. Zaro, W.C. Shen, Comparison of cationic and amphipathic cell penetrating peptides for siRNA delivery and efficacy, Mol. Pharm. 9 (2012) 299–309.

[10] H. Xia, X. Gao, G. Gu, Z. Liu, Q. Hu, Y. Tu, Q. Song, L. Yao, Z. Pang, X. Jiang, J. Chen, H. Chen, Penetratin-functionalized PEG-PLA nanoparticles for brain drug delivery, Int. J. Pharm. 436 (2012) 840–850.
[11] F. Heitz, M.C. Morris, G. Divita, Twenty years of cell-penetrating peptides: from molecular mechanisms to therapeutics, Br. J. Pharmacol. 157 (2009) 195–206.
[12] M. Tyagi, M. Rusnati, M. Presta, M. Giacca, Internalization of HIV-1 tat requires cell surface heparan sulfate proteoglycans, J. Biol. Chem. 276 (2001) 3254–3261.
[13] D. Derossi, S. Calvet, A. Trembleau, A. Brunissen, G. Chassaing, A. Prochiantz, Cell internalization of the third helix of the Antennapedia homeodomain is receptor-independent, J. Biol. Chem. 271 (1996) 18188–18193.
[14] A. Gautam, H. Singh, A. Tyagi, K. Chaudhary, R. Kumar, P. Kapoor, G.P. Raghava, CPPsite: A Curated Database of Cell Penetrating Peptides, Database (Oxford), bas015 (2012).
[15] G. Elliott, P. O'Hare, Intercellular trafficking and protein delivery by a herpesvirus structural protein, Cell 88 (1997) 223–233.
[16] D. Jha, R. Mishra, S. Gottschalk, K.H. Wiesmuller, K. Ugurbil, M.E. Maier, J. Engelmann, CyLoP-1: a novel cysteine-rich cell-penetrating peptide for cytosolic delivery of cargoes, Bioconjug. Chem. 22 (2011) 319–328.
[17] F. Milletti, Cell-penetrating peptides: classes, origin, and current landscape, Drug Discov. Today 17 (2012) 850–860.
[18] S. Futaki, T. Suzuki, W. Ohashi, T. Yagami, S. Tanaka, K. Ueda, Y. Sugiura, Arginine-rich peptides. An abundant source of membrane-permeable peptides having potential as carriers for intracellular protein delivery, J. Biol. Chem. 276 (2001) 5836–5840.
[19] M. Kosuge, T. Takeuchi, I. Nakase, A.T. Jones, S. Futaki, Cellular internalization and distribution of arginine-rich peptides as a function of extracellular peptide concentration, serum, and plasma membrane associated proteoglycans, Bioconjug. Chem. 19 (2008) 656–664.
[20] S. Futaki, Membrane-permeable arginine-rich peptides and the translocation mechanisms, Adv. Drug Delivery Rev. 57 (2005) 547–558.
[21] J.R. Maiolo, M. Ferrer, E.A. Ottinger, Effects of cargo molecules on the cellular uptake of arginine-rich cell-penetrating peptides, Biochim. Biophys. Acta 1712 (2005) 161–172.
[22] B. Christiaens, J. Grooten, M. Reusens, A. Joliot, M. Goethals, J. Vandekerckhove, A. Prochiantz, M. Rosseneu, Membrane interaction and cellular internalization of penetratin peptides, Eur. J. Biochem. 271 (2004) 1187–1197.
[23] D. Kalafut, T.N. Anderson, J. Chmielewski, Mitochondrial targeting of a cationic amphiphilic polyproline helix, Bioorg. Med. Chem. Lett. 22 (2012) 561–563.
[24] F. Madani, S. Lindberg, U. Langel, S. Futaki, G. A, Mechanisms of cellular uptake of cell-penetrating peptides, J. Biophys. 2011 (2011) 414729.
[25] A. Gautam, K. Chaudhary, R. Kumar, A. Sharma, P. Kapoor, A. Tyagi, G.P. Raghava, In silico approaches for designing highly effective cell penetrating peptides, J. Trans. Med. 11 (2013) 74.
[26] J.P. Richard, K. Melikov, E. Vives, C. Ramos, B. Verbeure, M.J. Gait, L.V. Chernomordik, B. Lebleu, Cell-penetrating peptides. A reevaluation of the mechanism of cellular uptake, J. Biol. Chem. 278 (2003) 585–590.
[27] P. Thevenet, Y. Shen, J. Maupetit, F. Guyon, P. Derreumaux, P. Tuffery, PEP-FOLD: an updated de novo structure prediction server for both linear and disulfide bonded cyclic peptides, Nucleic Acids Res. 40 (2012) W288–W293.
[28] W. Kabsch, C. Sander, Dictionary of protein secondary structure: pattern recognition of hydrogen-bonded and geometrical features, Biopolymers 22 (1983) 2577–2637.
[29] G. Tunnemann, G. Ter-Avetisyan, R.M. Martin, M. Stockl, A. Herrmann, M.C. Cardoso, Live-cell analysis of cell penetration ability and toxicity of oligo-arginines, J. Pept. Sci. 14 (2008) 469–476.
[30] R. Pasqualini, E. Koivunen, E. Ruoslahti, Alpha v integrins as receptors for tumor targeting by circulating ligands, Nat. Biotechnol. 15 (1997) 542–546.
[31] E. Ruoslahti, RGD and other recognition sequences for integrins, Annu. Rev. Cell Dev. Biol. 12 (1996) 697–715.
[32] W. Li, A. Godzik, Cd-hit: a fast program for clustering and comparing large sets of protein or nucleotide sequences, Bioinformatics 22 (2006) 1658–1659.
[33] T. Teesalu, K.N. Sugahara, V.R. Kotamraju, E. Ruoslahti, C-end rule peptides mediate neuropilin-1-dependent cell, vascular, and tissue penetration, Proc. Natl. Acad. Sci. USA 106 (2009) 16157–16162.
[34] W.M. Yau, W.C. Wimley, K. Gawrisch, S.H. White, The preference of tryptophan for membrane interfaces, Biochemistry 37 (1998) 14713–14718.
[35] C. Bechara, M. Pallerla, Y. Zaltsman, F. Burlina, I.D. Alves, O. Lequin, S. Sagan, Tryptophan within basic peptide sequences triggers glycosaminoglycan-dependent endocytosis, FASEB J. 27 (2013) 738–749.
[36] H.A. Rydberg, M. Matson, H.L. Amand, E.K. Esbjorner, B. Norden, Effects of tryptophan content and backbone spacing on the uptake efficiency of cell-penetrating peptides, Biochemistry 51 (2012) 5531–5539.
[37] D. Derossi, A.H. Joliot, G. Chassaing, A. Prochiantz, The third helix of the Antennapedia homeodomain translocates through biological membranes, J. Biol. Chem. 269 (1994) 10444–10450.
[38] S.L. Fang, T.C. Fan, H.W. Fu, C.J. Chen, C.S. Hwang, T.J. Hung, L.Y. Lin, M.D. Chang, A novel cell-penetrating peptide derived from human eosinophil cationic protein, PLoS One 8 (2013) e57318.
[39] E. Eiriksdottir, K. Konate, U. Langel, G. Divita, S. Deshayes, Secondary structure of cell-penetrating peptides controls membrane interaction and insertion, Biochim. Biophys. Acta 1798 (2010) 1119–1128.
[40] S.C. Li, N.K. Goto, K.A. Williams, C.M. Deber, Alpha-helical, but not beta-sheet, propensity of proline is determined by peptide environment, Proc. Natl. Acad. Sci. USA 93 (1996) 6676–6681.
[41] C.N. Pace, J.M. Scholtz, A helix propensity scale based on experimental studies of peptides and proteins, Biophys. J. 75 (1998) 422–427.
[42] L. Cascales, S.T. Henriques, M.C. Kerr, Y.H. Huang, M.J. Sweet, N.L. Daly, D.J. Craik, Identification and characterization of a new family of cell-penetrating peptides: cyclic cell-penetrating peptides, J. Biol. Chem. 286 (2011) 36932–36943.
[43] S.D. Conner, S.L. Schmid, Regulated portals of entry into the cell, Nature 422 (2003) 37–44.
[44] L.H. Wang, K.G. Rothberg, R.G. Anderson, Mis-assembly of clathrin lattices on endosomes reveals a regulatory switch for coated pit formation, J. Cell Biol. 123 (1993) 1107–1117.
[45] S.K. Rodal, G. Skretting, O. Garred, F. Vilhardt, B. van Deurs, K. Sandvig, Extraction of cholesterol with methyl-beta-cyclodextrin perturbs formation of clathrin-coated endocytic vesicles, Mol. Biol. Cell 10 (1999) 961–974.
[46] F. Duchardt, M. Fotin-Mleczek, H. Schwarz, R. Fischer, R. Brock, A comprehensive model for the cellular uptake of cationic cell-penetrating peptides, Traffic 8 (2007) 848–866.
[47] J.A. Gomez, J. Chen, J. Ngo, D. Hajkova, I.J. Yeh, V. Gama, M. Miyagi, S. Matsuyama, Cell-penetrating penta-peptides (CPP5s): measurement of cell entry and protein-transduction activity, Pharmaceuticals (Basel) 3 (2010) 3594–3613.
[48] C. O'Brien, D.R. Flower, C. Feighery, Peptide length significantly influences in vitro affinity for MHC class II molecules, Immun. Res. 4 (2008) 6.
[49] K. Numata, J. Hamasaki, B. Subramanian, D.L. Kaplan, Gene delivery mediated by recombinant silk proteins containing cationic and cell binding motifs, J. Controlled Release 146 (2010) 136–143.
[50] M. Oba, S. Fukushima, N. Kanayama, K. Aoyagi, N. Nishiyama, H. Koyama, K. Kataoka, Cyclic RGD peptide-conjugated polyplex micelles as a targetable gene delivery system directed to cells possessing alphavbeta3 and alphavbeta5 integrins, Bioconjug. Chem. 18 (2007) 1415–1423.
[51] I. Nakase, H. Hirose, G. Tanaka, A. Tadokoro, S. Kobayashi, T. Takeuchi, S. Futaki, Cell-surface accumulation of flock house virus-derived peptide leads to efficient internalization via macropinocytosis, Mol. Ther. 17 (2009) 1868–1876.
[52] C.E. Caesar, E.K. Esbjorner, P. Lincoln, B. Norden, Membrane interactions of cell-penetrating peptides probed by tryptophan fluorescence and dichroism techniques: correlations of structure to cellular uptake, Biochemistry 45 (2006) 7682–7692.
[53] P.A. Wender, D.J. Mitchell, K. Pattabiraman, E.T. Pelkey, L. Steinman, J.B. Rothbard, The design, synthesis, and evaluation of molecules that enable or enhance cellular uptake: peptoid molecular transporters, Proc. Natl. Acad. Sci. USA 97 (2000) 13003–13008.
[54] S. Console, C. Marty, C. Garcia-Echeverria, R. Schwendener, K. Ballmer-Hofer, Antennapedia and HIV transactivator of transcription (TAT) "protein transduction domains" promote endocytosis of high molecular weight cargo upon binding to cell surface glycosaminoglycans, J. Biol. Chem. 278 (2003) 35109–35114.
[55] J.P. Richard, K. Melikov, H. Brooks, P. Prevot, B. Lebleu, L.V. Chernomordik, Cellular uptake of unconjugated TAT peptide involves clathrin-dependent endocytosis and heparan sulfate receptors, J. Biol. Chem. 280 (2005) 15300–15306.
[56] S. Futaki, I. Nakase, A. Tadokoro, T. Takeuchi, A.T. Jones, Arginine-rich peptides and their internalization mechanisms, Biochem. Soc. Trans. 35 (2007) 784–787.